31st Annual International Conference of the IEEE EMBS
Minneapolis, Minnesota, USA, September 2-6, 2009

Molecular Therapeutic Agents for Noninvasive Photoacoustic Image-guided Photothermal Therapy

Pratixa P. Joshi, Yun-Sheng Chen, Seungsoo Kim, Jignesh Shah,
Konstantin Sokolov, and Stanislav Emelianov, *Member, IEEE*

***Abstract*—Gold nanoparticles are attracting increasing attention in nanomedicine due to their inherently low toxicity and unique optical properties. In particular, gold nanorods have been used in the thermal therapy due to their tunable strong longitudinal plasmon resonance in the near infra-red region and high conversion efficiency from optical to thermal energy. In this study we explore the potential of gold nanorods for photoacoustic image-guided photothermal therapy to treat cancers. We synthesize the gold nanorods and make them biocompatible by replacing the cytotoxic surfactant used in the synthesis (cetyl trimethyl ammonium bromide) with a biocompatible molecule and then demonstrate the targeting to the cancer cells by bioconjugation of the modified nanorods.**

I. Introduction

Current techniques for cancer treatment, such as chemotherapy, are not specific to the disease site and introduce significant damage to the healthy tissues of the body while treating the disease. An effective way to treat diseases such as cancers is to specifically label the cancerous area with diagnostic agents, treating the malignant region and leaving the healthy tissues unaffected by the treatment. Plasmonic enhanced photothermal therapy is used to noninvasively treat various medical conditions including cancers [1, 2]. Gold nanoparticles are of particular importance due to their unique optical properties. Our group has previously demonstrated that the absorption peak of the bioconjugated nanospheres attached to the cancer cells is broadened and slightly red-shifted due to the plasmon coupling of nanospheres attached to the cancer cells [3]. This provides an opportunity to differentiate targeted and nontargeted nanoparticles by detecting the photoacoustic signal at different wavelengths. However, spherical gold nanoparticles have a peak absorbance at a 530 nm wavelength, at which blood also absorbs significantly. To minimize the interference from blood, it is desirable to design contrast agents that absorb in the near infra-red region. The longitudinal absorption peak of the gold nanorods is dependent on their aspect ratio (length-to-diameter ratio); hence, it can be easily controlled by changing the size of the nanorods.

Ultrasound and photoacoustic imaging techniques can be used to monitor thermal therapy [4-6]. First, specifically targeted gold nanoparticles are used to label the cancer cells; then, the laser light is applied which is absorbed by the gold nanoparticle causing thermal expansion and generation of the acoustic waves. The photoacoustic waves are then detected using a multi-wavelength photoacoustic technique [3]. The therapy session which follows the photoacoustic imaging procedure applies higher intensity electromagnetic radiation. The gold nanorods, due to their higher optical absorption relative to the surrounding tissue, gain higher temperatures and selectively destroy the cancer cells.

The previous studies (Figure 1) have demonstrated that photoacoustic technique in combination with gold nanoparticles is an efficient way to detect the tumor cells, monitor thermal therapy and selectively ablate malign tumor tissue [6]. It is envisioned that the developed technique would provide clinicians with a tool to actively monitor anatomical and functional information to facilitate the cancer therapy.

The use of biocompatible gold nanorods for photothermal therapy has been reported [7, 8]. However, to improve the effectiveness of both thermal therapy and photoacoustic

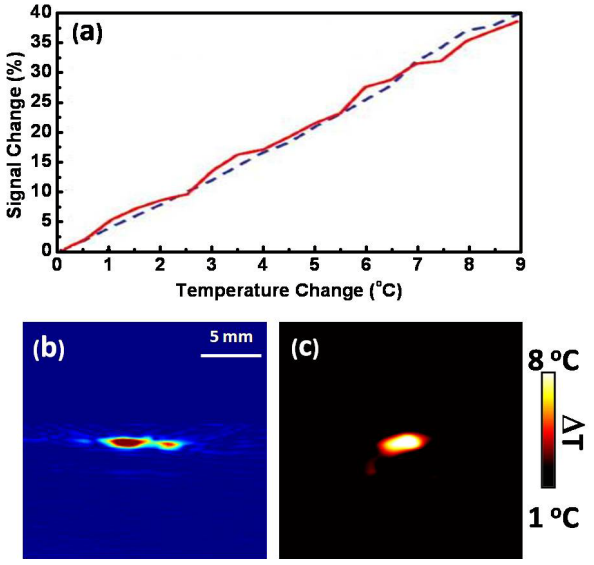

Fig. 1. (a) Photoacoustic signal change for a 9°C temperature increase in phantoms with and without photoabsorbing nanoparticles. Photothermal therapy experiment performed on porcine tissue with injected nanoparticles: (b) photoacoustic image, (c) photoacoustic based thermal image. (adapted from Shah et. al. [6])

Manuscript received April 7, 2009. This work was supported in part by the National Institutes of Health under grants EB 008101 and EB 008821.

Y.-S. Chen is with the Department of Electrical and Computer Engineering, University of Texas at Austin, Austin, TX 78712 USA (email: yunshengchen@gmail.com).

P. Joshi, S. Kim, J. Shah, K. Sokolov and S. Emelianov* are with the Department of Biomedical Engineering, University of Texas at Austin, Austin, TX 78712 USA (email: joshi@mail.utexas.edu, kim.seungsoo@mail.utexas.edu, konstantin.sokolov@engr.utexas.edu and corresponding author e-mail: emelian@mail.utexas.edu).

J. Shah is now with Volcano Inc., Rancho Cordova, CA 95670 (e-mail: jshah@volcanocorp.com).

thermal imaging, a specific design of a biofunctional gold nanorod is desired. In this study, the nanorods were modified from cetyl trimethylammonium bromide (CTAB)-coated gold nanorods via ligand exchange and 1-Ethyl-3-[3-dimethyl-aminopropyl]carbodiimide hydrochloride (EDC) mediated coupling reaction to produce immune-targeted gold nanorods. The cytotoxicity and targeting effectiveness of the nanorods have also been studied using the skin cancer cells.

II. Photoacoustic Thermal Imaging

Photoacoustic pressure or stress wave is generated by the thermo-elastic expansion of the objects absorbing the energy of the applied short electromagnetic pulse. From the generalized Hook's law, the fractional volume expansion dV/V can be expressed as:

$$\frac{dV(\vec{r},t)}{V} = -kP(\vec{r},t) + \beta T(\vec{r},t) \quad (1)$$

where k [Pa^{-1}] is the isothermal compressibility, β [K^{-1}] is the thermal expansion coefficient, and $P(\vec{r},t)$ [Pa], $T(\vec{r},t)$ [K] are the change of pressure and temperature at position $\vec{r}$, respectively. The isothermal compressibility can be expressed as [9]

$$k = \frac{C_p}{\rho c_s^2 C_v} \quad (2)$$

where ρ [g/cm^3] denotes the mass density, c_s is the speed of sound in the medium; C_p and C_v [J g^{-1} K^{-1}] represent the specific heat capacities at constant pressure and volume, respectively.

When the pulse is short, i.e., shorter than thermal relaxation and stress relaxation time, the excitation is thermal and stress confined which means the heat conduction and stress propagation are negligible. Under such conditions, the fractional volume of expansion is insignificant and the local electromagnetic pressure rises immediately after exposure, which can be derived from equation (1)

$$P(z) = \frac{\beta T(z)}{k} = \frac{\beta}{k}\frac{\eta_{th}\mu_a F(z)}{\rho C_v} \quad (3)$$

where η_{th} denotes the percentage of exposed energy converted to heat; μ_a [cm^{-1}] and $F(z)$ [J cm^{-2}] indicate the absorption coefficient of the medium and the local laser fluence, respectively. The local laser fluence depends on the initial laser fluence, F_0 [J cm^{-2}], attenuation of the optical radiation in the medium, $e^{-\mu_a z}$, and scattering coefficient of the medium, α_s. Thus, the pressure rise can be expressed as:

$$P(z) = \frac{\beta v_s^2}{C_p}\eta_{th}\mu_a F_0 \alpha_s e^{-\mu_{eff} z} = \Gamma \eta_{th}\mu_a F_0 \alpha_s e^{-\mu_{eff} z} \quad (4)$$

where $\Gamma = \beta c_s^2/C_p$ [dimensionless] is the Grüneisen coefficient. Specific heat capacity at constant pressure C_p and speed of sound c_s are both temperature dependent and linearly proportional to the temperature for water-based and fat-based tissues between 10 and 55°C [6]. Accordingly, the Grüneisen parameter is linearly dependent on the temperature in this region and is described as [4]

$$\Gamma = A + BT \quad (5)$$

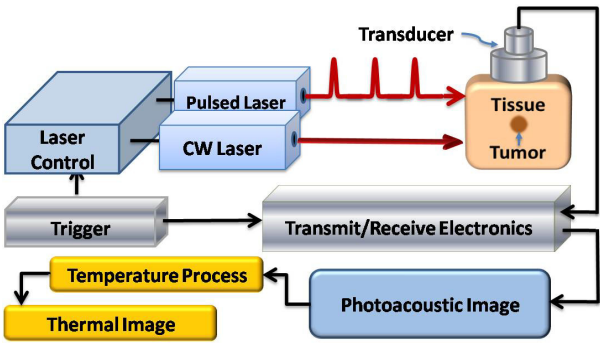

Figure 2. A block diagram illustrates the experimental setup for photoacoustic image- guided photo thermal therapy.

where A and B are constant and T is the equilibrium temperature of the measuring area. By substituting equation (5) in equation (4), and rearranging, we can write

$$\Delta T = a\frac{\Delta P}{P} \quad (6)$$

where a is a tissue dependent constant and can be determined experimentally. Photoacoustic thermal images are acquired using the equation above by converting the change of normalized photoacoustic signal amplitude to the change of temperature as shown in Fig. 1(a). Figures 1(b) and 1(c) illustrate a photoacoustic image and thermal image during photothermal therapy experiment performed on porcine tissue with injected nanoparticles.

III. Materials and Methods

A. Experimental Setup

An integrated imaging and therapeutic system was developed for photoacoustic image-guided photothermal therapy. The experimental setup is shown schematically in Fig. 2. A 38-mm aperture, 128 element linear array transducer operating at 5 MHz center frequency (SonicRP, Ultrasonix Medical Corporation, Canada) was used to capture ultrasound pulse-echo and photoacoustic transients. An OPO pulsed laser system (Vibrant B, Opotek Inc., USA), was used for photoacoustic imaging of tissue samples (800 nm wavelength, 5 ns pulse duration, 10 Hz repetition rate, up to 15 mJ/cm^2 optical fluence) An Nd:YAG pulsed laser (Polaris II, New Wave Research, Inc., USA) was used in the tissue-mimicking phantom experiments (532 nm wavelength, 5 ns pulse duration, 20 Hz repetition rate). Another continuous wave diode laser (HAM, Power Technology, Inc., USA) operating at 800 nm with a maximum power of 1 W, was used as a light source for the photothermal therapy.

During imaging, the sample was first irradiated by a pulsed laser, and the photoacoustic response was received on each element of the transducer array. Immediately after the photoacoustic imaging, conventional pulse-echo ultrasound imaging was performed. During the photothermal therapy, the phantom was irradiated using the CW diode laser, the photoacoustic frames were recorded every 10 seconds. The captured data was stored offline for temperature processing.

The experiments were performed at a room temperature of approximately 25°C.

B. Synthesis of Gold Nanorods

A seed-mediated growth of gold nanorods, first proposed by Murphy group [10] and later modified by El-Sayed group [11], was used. The protocol is briefly described as follows: 5 mL of CTAB solution (0.20 M) was first mixed with 5 mL of $HAuCl_{4(aq)}$ solution (0.5 mM). Then, 0.60 mL of ice-cold $NaBH_{4(aq)}$ solution (0.01 M) was added to the mixture, which resulted in the formation of a brownish yellow seed solution. The seed solution was vigorously stirred for 2 min at 25 °C.

The growth solution was made by adding 0.15-0.2 mL $AgNO_{3(aq)}$ (4 mM) solution to 5 mL of CTAB (0.20 M) solution. Five mL of $HAuCl_{4(aq)}$ (1 mM) was added to the mixture. After gentle mixing of the solution, 70 µL of ascorbic acid (0.0788 M) was added which resulted in the colorless growth solution. To grow nanorods, 12 µL of the seed solution was added to the growth solution at 27-30°C. The color of the solution changed within 10-20 min. The solution then aged for another 12 hours at 27-30°C. This technique produced nanorods with aspect ratios 3.8 to 4.4. The solution was centrifuged in the sequence of 18000 (G) for 45 min twice. The collected nanorods were re-dispersed to ultra pure water (18 mΩ) with concentration 1 mg to 1 mL water.

C. Modification of Gold Nanorods

The gold nanorods were modified to replace CTAB with 11-mercaptoundecanoic acid (MUDA) using the procedure developed by Yu et.al. [8]. Briefly, the as-prepared nanorods were twenty-times concentrated and washed with water using centrifugation. Five mL of the concentrated nanorods dispersed in water was mixed with 1 mL of MUDA solution (20 mM) in ethanol and sonicated at 50°C for 30 minutes. Then the solution was sonicated for 2 hours at 25°C. The mixture was then centrifuged at 5600 (G) for 5 mins. The modified nanorods were collected and dispersed in 10 mL of water.

D. Bioconjugation of Modified Gold Nanorods

The gold nanorods with MUDA (MUDA-NRs) were conjugated with antibodies using EDC-mediated coupling reaction. In short, the carboxylic acid groups on MUDA-NRs were activated by incubating MUDA-NRs suspension in 0.1 M sodium phosphate buffer (pH 5.5) with EDC and N-hydroxysulfosuccinimide (Sulfo-NHS) for 6 hours at room temperature. Then the unreacted EDC/Sulfo-NHS was removed by centrifugation. The nanorod pellets were then dispersed in 0.1 M sodium phosphate buffer (pH 7) and incubated with clone 29.1 antibodies overnight at room temperature. Bioconjugated nanorods were collected as a pellet after centrifugation.

E. Cytotoxicity and Cell Targeting Study with Modified Gold Nanorods

The cell viability test of human epithelial cancer cells (A431 cells) was performed using MTS (3-(4,5-dimethylthiazol-2-yl)-5-(3-carboxymethoxyphenyl)-2-(4-sulfophenyl)-2H-tetrazolium) cell viability assay.

To test targeting efficacy of bioconjugated nanorods, the A431 cells were incubated with MUDA-NRs attached to antibody for 6 hours at 37°C and then fixed with formalin. The dark field optical microscopy was performed to confirm labeling of the cells with nanoparticles.

IV. Results and Discussion

The photoacoustic signal strength and the efficiency of thermal therapy rely on the absorption strength of the gold nanorods at an excitation wavelength. To achieve maximum photoacoustic signal and effective thermal therapy, it is desirable to control the wavelength of absorption maximum (longitudinal band) of the gold nanorods to match the excitation wavelength of laser radiation. The plasmon resonance can be easily controlled by varying the aspect ratios (length-to-diameter ratio) of gold nanorods. Different aspect ratios of gold nanorods have been synthesized by varying the ratio of the concentration of gold ion (Au^{3+}) with respect to the concentration of silver nitrite. Figures 3(a) and 3(b) illustrate the transmission electron micrographs of the gold nanorods with average aspect ratio of 3.8 and 4.4, respectively. The UV-Vis spectroscopy study, as shown in Fig. 3(c), indicates four sets of gold nanorods whose plasmon longitudinal bands are from 770 nm to 820 nm with 15 nm interval. It provides enough coverage over the wavelength range to match laser diode radiation wavelength. The full width at half maximum (FWHM) of the longitudinal bands is within the range of 131±8 nm, which combined with TEM images suggests that the size distribution is similar for each set of gold nanorods.

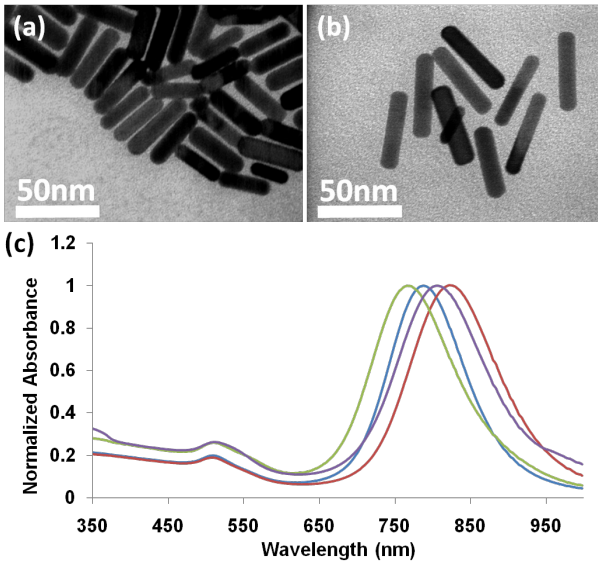

Fig. 3. TEM images illustrate the CTAB-coated gold nanorods with aspect ratio of (a) 3.8 and (b) 4.4. (c) The normalized absorbance spectra of CTAB-coated gold nanorods show that absorption maximum wavelengths are able to tune in the range from 770 nm to 820 nm.

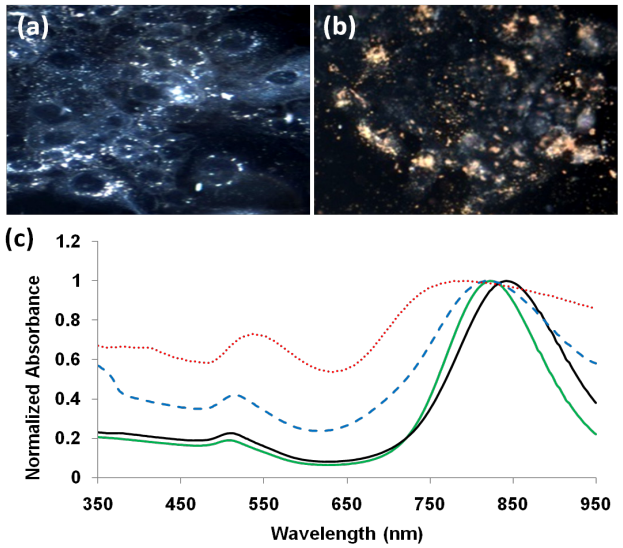

Fig. 4. Dark field microscopic images show (a) human skin A431 cancer cells and (b) cells with 29.1 antibody functionalized gold nanorods attached. (c) Normalized absorbance spectrum of gold nanorods denote that the absorptions of (green solid line) CTAB-coated gold nanorods; (black solid line) MUDA-coated gold nanords; (blue dashed line) the MUDA-coated gold nanorods dispersed in phosphate media, and (red dotted line) antibody functionalized gold nanorods, respectively.

The cytotoxicity of CTAB-coated gold nanorods has been reported by Murphy *et al.* [12]. The toxicity comes from the free CTAB molecules that are dissociated from the bilayer formed on the nanorods surface. For biological application, it is necessary to replace CTAB with other biocompatible molecules. In this study, CTAB was replaced by MUDA through ligand exchange reaction. The toxicity test was performed on both CTAB-gold nanorods and MUDA-coated gold nanorods. After four hours of incubation of an A431 cell with MUDA-coated gold nanorods, the number of viable A431 cells was at the same order of magnitude as the cells without any gold nanorods. But with CTAB-coated gold nanorods, most of the cells were dead. The MUDA-coated gold nanorods were further functionalized by an antibody. During functionalization, the carboxylic group of MUDA conjugated to amine group of the antibody to form an amide bond with the EDC-mediated coupling reaction. The antibody conjugated gold nanorods that were selectively immobilized on the A431 cells to test the targeting efficiency. The dark field optical microcopy images, as in Fig. 4(a) and 4 (b), show the cells without and with molecular specific nanorods, respectively. The golden color aggregate in the cell regions indicates the nanorods can be effectively targeted to the specific biomarker on the cancer cells. Fig. 4(c) shows the UV-Vis spectrum of gold nanorods recorded in each step of modification. The black curve shows the normalized absorption spectrum of nanorods in water after replacement of CTAB with MUDA, the absorption peak slightly shifts from that of the CTAB-coated nanorods, because of the change of the surrounding dielectric constant [8]. The blue and red curves in Figure 4(c) represent the spectra of MUDA-NRs re-dispersed in phosphate buffer and of the antibody functionalized gold nanorods, respectively. The broadening of the absorption peak could be caused by the aggregation of gold nanorods while conjugated with antibodies. This aggregation can be eliminated by reducing the incubation time with antibodies during the conjugation process.

V. Conclusion

Biocompatible targeted gold nanorods have been developed by modifying CTAB-coated gold nanorods via ligand exchange and EDC-mediated coupling reaction. The targeting effectiveness of the nanorods to the skin cancer cells has also been demonstrated in this study, which can be used to develop molecule-specific therapeutic agents for noninvasive photoacoustic imaging and photothermal therapy. The strong longitudinal absorption maximum which can be fine-tuned to match the wavelength of the laser radiation is expected to provide improved effectiveness for thermal therapy and an optimized signal for photoacoustic thermal imaging.

References

[1] X. H. Huang, I. H. El-Sayed, W. Qian, and M. A. El-Sayed, "Cancer cell imaging and photothermal therapy in the near-infrared region by using gold nanorods," *Journal of the American Chemical Society,* vol. 128, pp. 2115-2120, Feb 2006.

[2] J. L. West and N. J. Halas, "Engineered nanomaterials for biophotonics applications: Improving sensing, imaging, and therapeutics," *Annual Review of Biomedical Engineering,* vol. 5, pp. 285-292, 2003.

[3] S. Mallidi, T. Larson, J. Aaron, K. Sokolov, and S. Emelianov, "Molecular specific optoacoustic imaging with plasmonic nanoparticles," *Optics Express,* vol. 15, pp. 6583-6588, May 2007.

[4] I. V. Larina, K. V. Larin, and R. O. Esenaliev, "Real-time optoacoustic monitoring of temperature in tissues," *Journal of Physics D-Applied Physics,* vol. 38, pp. 2633-2639, Aug 2005.

[5] J. Shah, S. R. Aglyamov, K. Sokolov, T. E. Milner, and S. Y. Emelianov, "Ultrasound imaging to monitor photothermal therapy - Feasibility study," *Optics Express,* vol. 16, pp. 3776-3785, Mar 2008.

[6] J. Shah, S. Park, S. Aglyamov, T. Larson, L. Ma, K. Sokolov, K. Johnston, T. Milner, and S. Y. Emelianov, "Photoacoustic imaging and temperature measurement for photothermal cancer therapy," *Journal of Biomedical Optics,* vol. 13, p. 9, May-Jun 2008.

[7] X. H. Huang, P. K. Jain, I. H. El-Sayed, and M. A. El-Sayed, "Plasmonic photothermal therapy (PPTT) using gold nanoparticles," *Lasers in Medical Science,* vol. 23, pp. 217-228, Jul 2008.

[8] C. X. Yu, L. Varghese, and J. Irudayaraj, "Surface modification of cetyltrimethylammonium bromide-capped gold nanorods to make molecular probes," *Langmuir,* vol. 23, pp. 9114-9119, Aug 2007.

[9] A. A. Oraevsky, S. L. Jacques, and F. K. Tittel, "Measurement of tissue optical properties by time-resolved detection of laser-induced transient stress," *Applied Optics,* vol. 36, pp. 402-415, Jan 1997.

[10] N. R. Jana, L. Gearheart, and C. J. Murphy, "Seed-mediated growth approach for shape-controlled synthesis of spheroidal and rod-like gold nanoparticles using a surfactant template," *Advanced Materials,* vol. 13, pp. 1389-1393, Sep 2001.

[11] B. Nikoobakht and M. A. El-Sayed, "Preparation and growth mechanism of gold nanorods (NRs) using seed-mediated growth method," *Chemistry of Materials,* vol. 15, pp. 1957-1962, May 2003.

[12] C. J. Murphy, A. M. Gole, J. W. Stone, P. N. Sisco, A. M. Alkilany, E. C. Goldsmith, and S. C. Baxter, "Gold Nanoparticles in Biology: Beyond Toxicity to Cellular Imaging," *Accounts of Chemical Research,* vol. 41, pp. 1721-1730, Dec 2008.